

Artículo de investigación

**Signal spectrum distortion for an extended target in a radar with a continuous frequency-modulated signal**

Искажение спектра сигнала протяженной цели в радаре с непрерывным частотно-модулированным сигналом

Distorsión del espectro de la señal del objetivo extendido en un radar de frecuencia modulada continua

Distorção do espectro do sinal do objetivo estendido em um radar de frequência modulada contínua

Recibido: 20 de abril de 2019. Aceptado: 07 de junio de 2019

Written by:

**Konstantin Yu. Gavrilov**<sup>67</sup>

<https://www.scopus.com/authid/detail.uri?authorId=7005242571>

**Kirill V. Kamenski**<sup>68</sup>

**Anatoly I. Kanaschenkov**<sup>69</sup>

<https://www.scopus.com/authid/detail.uri?origin=AuthorProfile&authorId=6508000443&zone=>

**Nadezhda S. Panyavina**<sup>70</sup>

**Abstract**

The problem of spectrum distortion in radar with a continuous frequency modulated signal (FMCW radar) is considered in the case of locating extended targets containing a large number of closely spaced reflection points. An extended target model is introduced for which a beat signal is analyzed based on its representation in the form of an amplitude-modulated oscillation. It is shown that the distortion of the spectrum occurs due to a certain relationship between the distances of the target points, the values of the carrier frequency and the deviation of the probe signal frequency. The results of numerical calculations for various values of the signal parameters and the long target model are given.

**Keywords:** extended target model, numerical calculations, radar, spectrum distortion.

**Аннотация**

Рассмотрена проблема искажения спектра в радаре с непрерывным частотно-модулированным сигналом (FMCW радаре) при лоцировании протяженных целей, содержащих большое число близкорасположенных точек отражения. Введена модель протяженной цели, для которой проведен анализ сигнала биений на основе представления его в виде амплитудно-модулированного колебания. Показано, что искажение спектра возникает в результате определенных соотношений между расстояниями точек цели, значениями несущей частоты и частоты девиации зондирующего сигнала. Приведены результаты численных расчетов для различных значений параметров сигнала и модели протяженной цели.

**Ключевые слова:** искажение спектра, модели протяженной цели, радар, численный расчёт.

<sup>67</sup> Doctor of Sciences, Deputy Head of Department, Moscow Aviation Institute (National Research University), 125080 Volokolamskoe highway 4, Moscow, Russia, gavr401.konst.y@mail.ru  
[https://elibrary.ru/author\\_items.asp?authorid=13560](https://elibrary.ru/author_items.asp?authorid=13560)

<sup>68</sup> Postgraduate student, Moscow Aviation Institute (National Research University), 125080 Volokolamskoe highway 4, Moscow, Russia, danonik92@mail.ru

<sup>69</sup> Doctor of Sciences, Professor, Head of Department, Moscow Aviation Institute (National Research University), 125080 Volokolamskoe highway 4, Moscow, Russia, kai@western-metal.ru  
[https://elibrary.ru/author\\_items.asp?authorid=336818](https://elibrary.ru/author_items.asp?authorid=336818)

<sup>70</sup> Postgraduate student, Moscow Aviation Institute (National Research University), 125080 Volokolamskoe highway 4, Moscow, Russia, danonik92@mail.ru

## Resumo

No presente artigo, o problema da distorção do espectro em radares com sinal de frequência modulada contínua (radar FMCW) é abordado ao produzir objetivos prolongados que contêm um grande número de pontos de reflexão próximos. O documento introduz um modelo objetivo estendido para o qual uma análise do sinal de batimentos cardíacos é realizada de acordo com sua apresentação na forma de uma oscilação de amplitude modulada. Este estudo mostra que a distorção do espectro ocorre como resultado de certas relações entre as distâncias dos pontos de destino, os valores da frequência da portadora e a frequência do desvio do sinal sonoro. O artigo apresenta os resultados dos cálculos numéricos para os diferentes valores dos parâmetros do sinal e do modelo objetivo estendido.

**Palavras-chave:** cálculos numéricos, distorção de espectro, modelo estendido, radar.

## Resumen

En el presente artículo se aborda el problema de la distorsión del espectro en radares con señal continua de frecuencia modulada (radar FMCW) al producir objetivos prolongados que contienen un gran número de puntos de reflexión cercanos. El documento introduce un modelo de objetivo extendido para el cual se realiza un análisis de la señal de los latidos en función de su presentación en forma de oscilación de amplitud modulada. Este estudio muestra que la distorsión del espectro se produce como resultado de ciertas relaciones entre las distancias de los puntos de destino, los valores de frecuencia portadora y la frecuencia de desviación de la señal de sondeo. El artículo presenta los resultados de los cálculos numéricos para los diferentes valores de los parámetros de la señal y el modelo de objetivo extendido.

**Palabras clave:** cálculos numéricos, distorsión del espectro, modelo extendido, radar.

## Introduction

Radars with a continuous frequency-modulated signal (Frequency-modulated continuous-wave (FMCW) radars, hereinafter FMCW radars) are characterized by a relatively short working distance and have a very wide range of applications as radio altimeters, territory protection radars, car radars, and long radio transparent media (gases, liquids, etc.) sensors, radars with aperture synthesis, and so on. In these radars, a linear sawtooth symmetric or asymmetric law of the carrier frequency variation is usually used, followed by a spectral analysis of the converted signal (beat signal) (Komarov & Smolsky, 2010; Kanashchenkov, Matveev, Minaev & Novikov, 2017).

The theory and technique of FMCW radars designing, including the reception and processing of signals, has been well studied. However, despite this, there is a phenomenon of signal spectrum distortion upon reflection from an extended target, which has not been adequately considered in the contemporary literature. This phenomenon, which is confirmed both by computer simulation and as a result of field experiments (Batet, Dios, Comeron & Agishev, 2010), occurs when locating long targets or in the presence of a group of point reflectors, the distance between which is comparable or less than the range resolution. An

analysis of such signals in the frequency domain was carried out and a method was proposed for processing the received signal when modifying the probing signal, which makes it possible to eliminate the spectrum distortion (Batet, Dios, Comeron & Agishev, 2010).

In the present work, the signal received from an extended target is analyzed in the time domain, which makes it possible to identify the causes of spectrum distortion associated with the phase relationships of individual point reflectors, as well as to determine the conditions under which such distortions arise. Conducting such an analysis on the basis of determining the type of the resulting signal, as well as identifying the conditions for useful signal spectrum distorting, is the goal of this work.

Determining the causes of signal distortion in the FMCW radar is very important in the formation of radar images (RI) by synthesizing an aperture. The formation of RI in such airborne radars, as well as their application for monitoring the earth surface are discussed in (Gavrilov, Kanashchenkov, Nuzhdin & Panyavina, 2018; Ananenko, Kanashchenkov, Nuzhdin, Rastorguev & Smolyar, July, 2017).

### Description of the signal from the extended target in the FMCW radar

Consider FMCW radar using periodic linear frequency modulation (LFM/chirp) with

symmetric and asymmetric frequency variation laws – see Figure 1a and 1b, respectively.

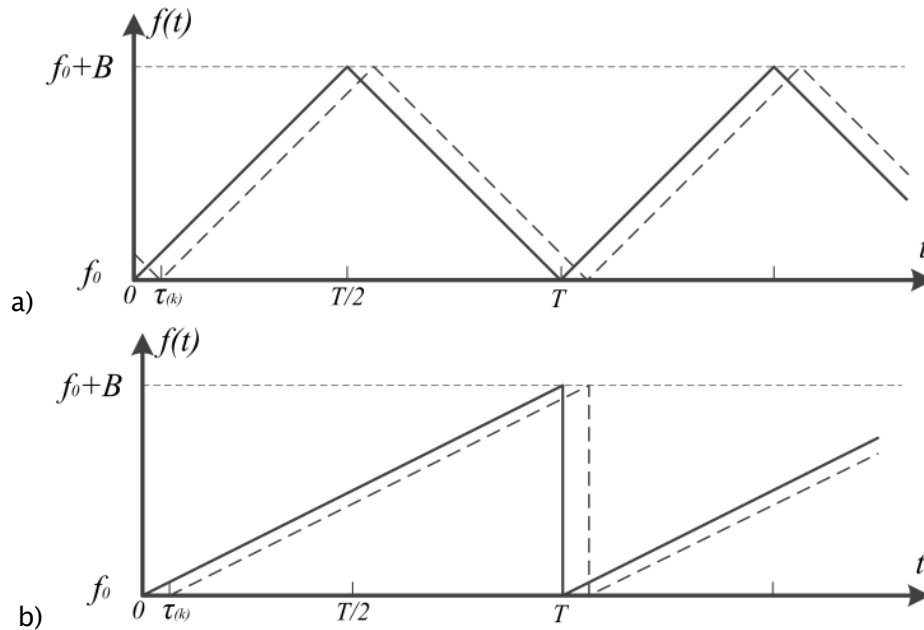


Figure 1. Laws of carrier frequency change in FMCW radar: a) - symmetric law; b) - asymmetric law

In Figure 1 is designated:  $T$  – is the modulation period;  $f_0$  – the initial frequency value;  $B$  – deviation (range of change) of frequency during one period. Dashed lines in Figure 1 represents the laws of frequency variation of the received signal, reflected from a point target and having a delay:

$$\tau^{(k)} = \frac{2R^{(k)}}{c}, \quad (1)$$

where  $R^{(k)}$  – distance to the target;  $c$  – radio wave propagation velocity.

Given the most widespread in FMCW radar practice signal with an asymmetric law (Figure 1b), as well as the identity of the analysis in both cases of the modulation, we will further consider the case of an asymmetric chirp signal, which for the duration of one period  $T$  can be written as:

$$s_t(t) = U_t \cos(2\pi f_0 t + \pi\beta t^2 + \varphi_0), \quad 0 \leq t \leq T, \quad (2)$$

where  $U_t$  – signal amplitude;  $\varphi_0$  – start signal phase;  $\beta = B/T$  – frequency increase slope.

Methods of receiving and processing the reflected signals to detect targets and measure their distance are described in detail in the literature (Komarov & Smolsky, 2010). Here we note that for a point target located at a distance  $R^{(k)}$ , the signal after all necessary conversions (converted signal) considering relation (2) and without taking noise into consideration takes the form (Gavrilov, Kanaschenkov, Nuzhdin & Panyavina, 2018):

$$s_r(t) = U_r^{(k)} \cos(2\pi F_6^{(k)} t + \theta^{(k)}), \quad (3)$$

where  $U_r^{(k)}$  – converted signal (CS) amplitude;

$$F_6^{(k)} = \beta\tau^{(k)} = \beta \frac{2R^{(k)}}{c} \quad (4)$$

– beat frequency;

$$\theta^{(k)} = 2\pi f_0 \tau^{(k)} - \pi\beta(\tau^{(k)})^2 + \varphi_0^{(k)} \quad (5)$$

– converted signal phase, where:

$$\varphi_0^{(k)} = \varphi_0 - \tilde{\varphi}_0^{(k)} \quad (6)$$

and  $\tilde{\varphi}_0^{(k)}$  – phase shift, arising when probing signal reflects from the target. The condition  $\tau^{(k)} \ll T$ , is usually satisfied in FMCW radars. Therefore, with sufficiently high accuracy, we can assume that expression (3) is valid for all  $t \in [0, T]$ .

Let us introduce a model of an extended target in the form of a set of  $K$  point reflectors uniformly spaced along the slant range with an  $\Delta R$  interval:

$$R^{(k)} = R_0 + (k - 1) \cdot \Delta R, \quad k = 1, \dots, K, \quad (7)$$

where  $R_0$  – distance to the nearest point of target (leading edge of the target);  $R^{(K)}$  – distance to the most remote point of the target (rear edge of the target). The value  $R_{\text{н}} = R^{(K)} - R_0$  determines the length of the target. For the considered target model, an important condition is the fact that the distance between adjacent points must be commensurate with or less than the radar resolution in terms of slant range, i.e.:

$$\Delta R \leq \Delta r, \quad (8)$$

where, as known,

$$\Delta r = \frac{c}{2B}. \quad (9)$$

Thus, the converted signal for the considered long target model can be written as follows:

$$s_r(t) = \sum_{k=1}^K U_r^{(k)} \cos(2\pi F_6^{(k)} t + \theta^{(k)}), \quad t \in [0, T], \quad (10)$$

where values  $F_6^{(k)}$  and  $\theta^{(k)}$  are calculated according to (4) and (5) considering (1), (7) and (8). An important feature of this model is the condition of constant phase  $\tilde{\varphi}_0^{(k)}$ ,  $k = 1, \dots, K$  that is valid for homogeneous targets.

Considering this, we will further assume that in (10) for the phases  $\theta^{(k)}$  (see (5) and (6)) the phase shifts are the same for all reflectors:

$$\varphi_0^{(k)} = \theta_0, \quad k = 1, \dots, K. \quad (11)$$

After passing through the balanced mixer converted signal is subjected to sampling operation and calculating the discrete Fourier transform (Komarov & Smolsky, 2010). The obtained CS spectrum is regarded as a range "portrait" of locating region.

Model (7), (10) was used in computer modeling of a long target signal. In this case, the values of the probing signal parameters were taken, the most common for FMCW radars of the centimeter wavelength range (Gavrilov, Kanaschenkov, Nuzhdin & Panyavina, 2018):

$$f_0 = 10 \text{ GHz}, \quad B = 150 \text{ MHz}, \quad T = 0,001 \text{ s}. \quad (12)$$

Note that the selected parameters values provide the slant range resolution  $\Delta r = 1$ . For an extended target, the following parameters were set:

$$R_0 = 1000 \text{ m}, \quad R_{\text{н}} = 20 \text{ m}, \quad \Delta R = 0,1 \dots 1 \text{ m}, \quad U_r^{(k)} = U_0, \quad k = 1, \dots, K. \quad (13)$$

The small length of the target relative to the distance to it causes, according to the basic radar equation, an almost uniform signal level over the entire length of the target: the amplitude deviations are within  $\approx 8\%$ . This circumstance allows within the range of the target length  $R_{\text{н}}$  to expect a uniform amplitude spectrum of CS, which is close to rectangular. However, the results of numerical calculations of the signal  $s_r(t)$  show that this is not so. Such results for given values of the signal and target parameters are presented in Figures 2-5 with values of  $\Delta R = 0.1; 0.3; 0.4; 0.5$  m, respectively: (a) – CS values for the duration of one period  $T$ ; (b) – values of the normalized amplitude spectrum of the CS. In Figures 2-5 b on the abscissa axis the values of the slant range are plotted, calculated on the basis of the beat frequencies according to (4). In these Figures, the dashed lines denote the signals of the sums of amplitude spectra obtained for each point reflector independently of each other. It can be said that the dashed lines are the desired responses from a long target, close to its real range "portrait".

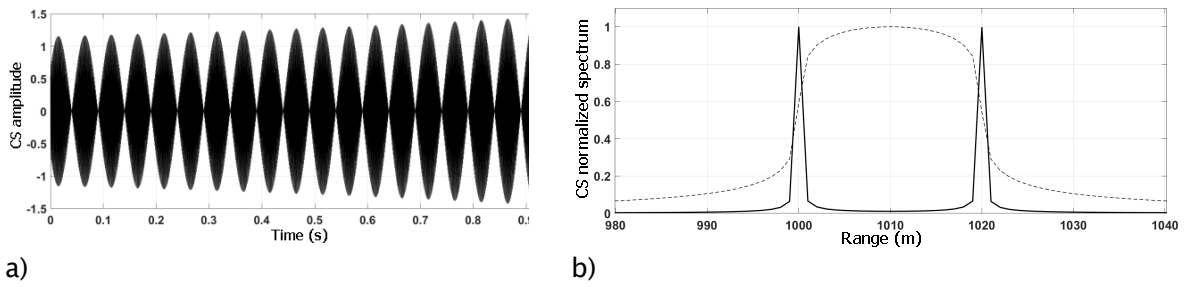


Figure 2. The value of CS (a) and spectrum of CS (b) at  $\Delta R = 0,1 \text{ m}$  ( $K = 200$ )

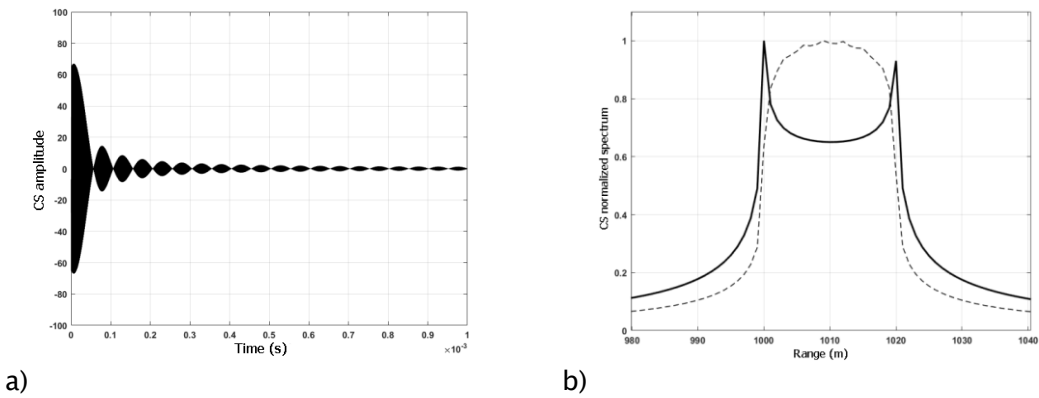


Figure 3. The value of CS (a) and spectrum of CS (b) at  $\Delta R = 0,3 \text{ m}$  ( $K = 67$ )

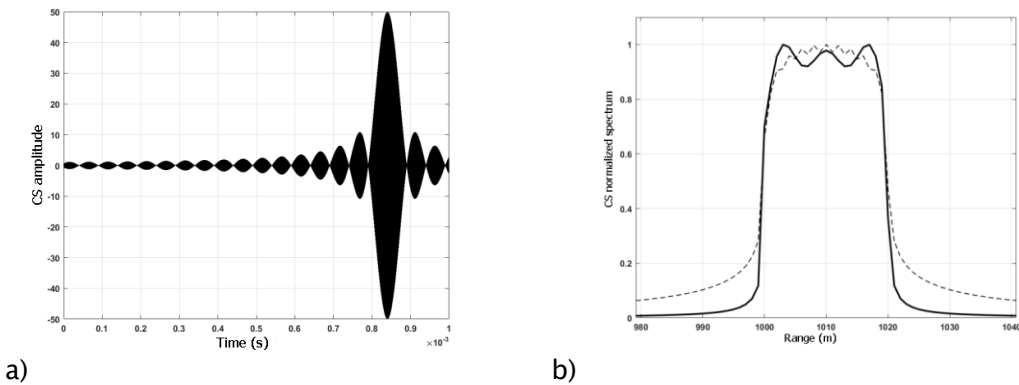


Figure 4. The value of CS (a) and spectrum of CS (b) at  $\Delta R = 0,4 \text{ m}$  ( $K = 50$ )

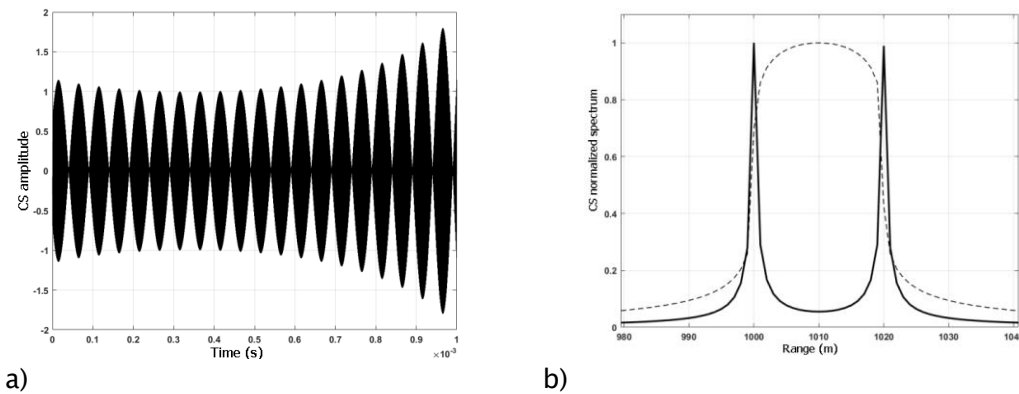


Figure 5. The value of CS (a) and spectrum of CS (b) at  $\Delta R = 0,5 \text{ m}$  ( $K = 40$ )

Amplitude CS spectra in Figures 2 b, 3 b, 5 b illustrate the distortion of the resulting signal spectrum, leading to a partial or complete loss of information about the internal structure of an extended target. In this case, the front and rear edges of the target are clearly detected. This distortion almost completely disappears at distances between adjacent points of reflection  $\Delta R = 0,4$  m (Figure 4b).

The presented results are consistent with similar results (Batet, Dios, Comeron & Agishev, 2010), obtained both in computer simulation and in field tests with a lidar using an FMCW signal with an asymmetric frequency variation law. The reason for the extended target converted signal spectrum distortion is the imposition of the responses of individual reflectors in such a way that individual frequency samples are added up with different phases. As known (Komarov & Smolsky, 2010), these individual reflectors responses have a type of sinc functions. It should be noted that such a distortion occurs only at certain values of the distances  $\Delta R$  and, as will be seen from further consideration depends on the values of the carrier frequency  $f_0$  and the frequency deviation B.

Further signal analysis (10) requires an assessment of the individual harmonics' parameters contribution – amplitudes and phases – to the resulting signal.

#### Extended target converted signal analysis

To analyze the signal  $s_r(t)$  (10), we will use the formula known from trigonometry:

$$\cos \alpha + \cos \gamma = 2 \cos \frac{1}{2}(\alpha + \gamma) \cos \frac{1}{2}(\alpha - \gamma), \quad (14)$$

which is applicable for each pair of harmonics from (10) with numbers  $(k=1, k=K)$ ,  $(k=2, k=K-1)$ , ... . Obviously, the factor  $\cos((\alpha + \gamma)/2)$  in (14) gives the same frequency value equal to the middle of the frequency interval of the beats of all points of an extended target (see (4) and (7)):

$$F_s = \frac{F_0^{(1)} + F_0^{(K)}}{2} = \frac{\beta}{2} \left( \tau_0 + \frac{K-1}{2} \Delta \tau \right), \quad (15)$$

where  $\tau_0 = \tau^{(1)} = 2R_0/c$ ,  $\Delta \tau = 2\Delta R/c$ ,  $\tau^{(k)} = \tau_0 + (k-1)\Delta \tau$ .

The phases of these factors are also the same (more precisely, almost the same), although this is not as obvious as for the frequency values. To verify this, consider the second term of the phase  $\theta^{(k)}$  in expression (5). Considering the condition  $\Delta \tau \ll \tau_0$ , we obtain

$$\pi \beta (\tau^{(k)})^2 \cong \pi \beta \tau_0^2 + 2\pi \beta \tau_0 (k-1) \Delta \tau, \quad (16)$$

it follows from this that the phases  $\theta^{(k)}$  are linear functions of the number k and in the case of the target homogeneity (see condition (11)) the phases of the harmonics of the first factors in (14) are equal to:

$$\theta_s = 2\pi f_0 \left( \tau_0 + \frac{K-1}{2} \Delta \tau \right) - \pi \beta \tau_0 (\tau_0 + (K-1) \Delta \tau) + \theta_0. \quad (17)$$

Using relations (4), (5), (11) and (16), it is also easy to obtain the values of the frequencies and phases of the difference of arguments in the second factor in (14):

$$F_r^{(k)} = \beta \Delta \tau \left( \frac{K+1}{2} - k \right), \quad \theta_r^{(k)} = 2\pi \Delta \tau \left( \frac{K+1}{2} - k \right) (f_0 - \beta \tau_0). \quad (18)$$

Thus, finally CS from an extended target of the form (10) can be written as:

$$s_r(t) = 2 \cos(2\pi F_s t + \theta_s) \sum_{k=1}^{K_2} \cos(2\pi F_r^{(k)} t + \theta_r^{(k)}), \quad t \in [0, T] \quad (19)$$

where  $K_2 = K/2$  or  $K_2 = (K-1)/2$  in the case of an even or odd value of K, respectively.

Relation (19) characterizes the function  $s_r(t)$  as an amplitude-modulated signal, in which the oscillation with frequency  $F_s$  is modulated by a relatively low-frequency oscillation:

$$S_M(t) = \sum_{k=1}^{K_2} \cos(2\pi F_r^{(k)} t + \theta_r^{(k)}), \quad t \in [0, T], \quad (20)$$

with  $F_r^{(k)} \ll F_s$ ,  $k = 1, \dots, K_2$ . It is convenient to analyze the signal  $S_M(t)$  for the limiting case when  $K_2 \rightarrow \infty$  with the unchanged value  $R_{II} = \text{const}$  (at the same time  $\Delta R \rightarrow 0$ ), when the sum in (20) converts into the integral:

$$S_M(t) = C_n \int_0^{F_r^{(K)}} \cos(2\pi f(t - t_0)) df = C_n \text{sinc}(2\pi F_r^{(K)}(t - t_0)), \quad (21)$$

where  $t_0 = \tau_0 - (f_0/\beta)$ ;  $C_n$  – normalization factor.

Thus, according to (21), the signal  $s_r(t)$  for sufficiently large  $K$  values approaches the function sinc, the amplitude spectrum of which, as is known (Gonorovsky, 1986), is close to a rectangular shape. This happens only when the maximum value of the function is reached in the central part of the probing chirp signal length, i.e. at  $t_0 \approx T/2$  (see (21)), which is possible with certain relations of  $\Delta\tau$ ,  $f_0$  and  $B$  values, which correspond to Figures 4a, b. Unlike Figures 2,3,5, in Figure 4, at  $\Delta R = 0,4$  m ( $\Delta\tau = 0,2667 \cdot 10^{-9}$  s), a function similar to sinc is observed, and in Figure 4b - amplitude spectrum corresponding to the undistorted form of an extended target reflectivity.

Using expression (20) it is possible to obtain conditions under which there is no distortion of the CS spectrum from an extended target for any values of  $K$ . A sinc-like signal that is symmetrical about the center of the pulse duration  $t_0 = T/2$  occurs when all the harmonics in (20) at a time  $t_0$  have the same phases, equal to the values of  $\pi n$ , where  $n = 1, 2, \dots$ . According to this condition and using (18) for the full phase of the  $k$ th harmonic in (20), we obtain the following:

$$2\pi\Delta\tau q_k(\beta t_0 + f_0 - \beta\tau_0) = \pi n, \quad n = 1, 2, \dots, \quad k = 1, \dots, K_2, \quad (22)$$

where  $q_k = \frac{K+1}{2} - k$ . Since for any value of  $k$  we have  $q_{k+1} - q_k = 1$  and the minimum value is  $q_K = q = 0,5$ , the conditions (22) for all values of  $k$  should be satisfied when  $2\pi\Delta\tau q \left( \beta \frac{T}{2} + f_0 - \beta\tau_0 \right) = \pi n$  or:

$$\Delta\tau \left( \frac{B}{2} + f_0 - \beta\tau_0 \right) = n. \quad (23)$$

According to  $\tau_0 \ll T/2$ , we will finally get:  
 $\Delta\tau = \frac{n}{f_0 + \frac{B}{2}}$  or  $\Delta R = \frac{cn}{2f_0 + B}$  when  $n = 1, 2, \dots$ .

$$(24)$$

Relation (24) determines the conditions under which there are no distortions of the CS spectrum from an extended target. It should be noted that the complete absence or the presence of small distortions will be observed in a certain range of intervals near the values of  $\Delta R$  ( $n = 1, 2, \dots$ ), corresponding to the sinc function maximum positions on the time axis within a certain interval  $t_1 < \frac{T}{2} < t_2$  with an allowable level of spectrum distortion.

The Table 1 for two values of the frequency deviation  $B$  presents the results of calculations of the inter-point distances of the extended target, implemented according to (24).

Table 1. Estimated values of inter-point intervals at which there are no distortions of the CS spectrum

Signal parameters: $f_0 = 10$ GHz, $T = 0,001$ sec, $B = 150$ MHz						
n	1	5	10	20	30	40
(m) $\Delta R$	0,014888	0,07444	0,14888	0,29776	0,44664	0,59552
Signal parameters: $f_0 = 10$ GHz, $T = 0,001$ sec, $B = 100$ MHz						
n	1	5	10	20	30	40
(m) $\Delta R$	0,014925	0,074625	0,14925	0,2985	0,44775	0,597

From the table, it can be seen that with the frequency deviation  $B=150$  MHz, the absence of spectrum distortion is possible. For example, with the inter-point distance  $\Delta R = 0,29776$  m ( $n = 20$ ). However, a very slight increase in this distance to the value of  $\Delta R = 0,3$  m already leads to a significant spectrum

distortion, which is illustrated in Figure 3b. In this case, the number of point reflectors  $K$  can be any.

The absence of distortions in the CS amplitude spectrum for the calculated values of  $\Delta R = 0,14888$  m ( $n = 10$ ) and  $\Delta R = 0,44664$  m ( $n =$

30) is illustrated in Figures 6b, 7b. Signals in Figures 6a, 7a, calculated for the number of reflection points  $K=50$ , are close in shape to the

sinc function located in the middle of the  $[0, T]$  interval, and their amplitude spectra (Figures 6b, 7b) have an almost rectangular form.

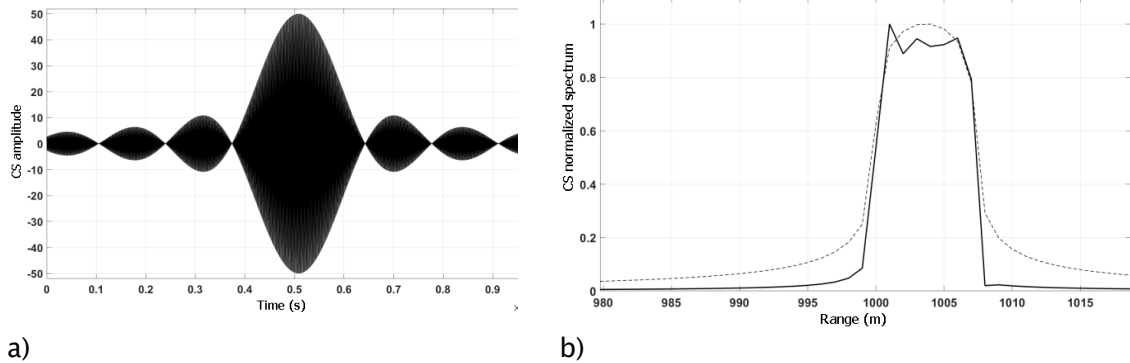


Figure 6. The value of CS (a) and spectrum of CS (b) at  $\Delta R = 0,14888$  m

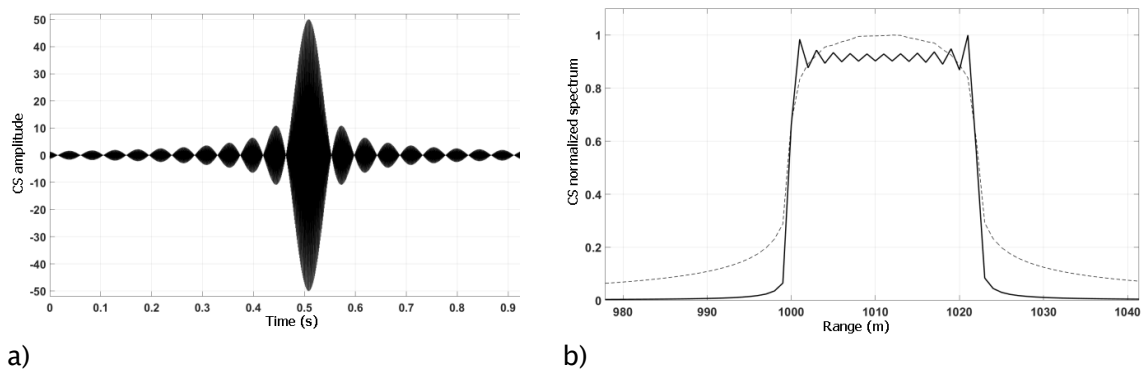


Figure 7. The value of CS (a) and spectrum of CS (b) at  $\Delta R = 0,44664$  m

An analysis of relations (24) shows that significant (by 1.5 ... 2 times) changes in the deviation of frequency  $B$  lead to very insignificant changes in the distances  $\Delta R$  – within tenths of percent. The carrier frequency  $f_0$  (assuming  $f_0 \gg B$ ) has the greatest effect on  $\Delta R$  values: its relative changes lead to almost the same relative changes in  $\Delta R$  values.

### Conclusion

It is noted that in the practice of using radars with a continuous frequency-modulated signal (FMCW radars) there is a phenomenon of distortion of the reflection coefficient for an extended target. The dimensions of this target should exceed the radar resolution in slant range. This property express itself in the distortion of the amplitude spectrum shape of the converted signal (beat signal), which in the case of a target that is uniform by range, should have the shape of a rectangle.

To study the causes of such a distortion, a model of an extended target was introduced in the form of a set of a large number of point reflectors, the distance between which should be commensurate with or be less than the radar resolution in range. Based on the introduced model, numerical calculations were used to obtain examples of signals reflected from extended targets, illustrating the different degrees of the amplitude spectrum deviation from the desired shape.

In the time domain, an analysis of the transformed signal obtained upon reflection from an extended target was carried out. The analysis is based on the representation of a signal in the form of an amplitude-modulated oscillation and the determination of the phase relationships of low-frequency harmonics (modulating function), at which the detected spectrum distortion occurs. It is shown that, with an increase in the number of reflection points, the considered signal approaches the sinc function, whose amplitude spectrum has a rectangular shape only if the maximum of this function is found within the

duration of the chirp repetition period. Based on the performed analysis, the relationships between the inter-point distances of the target, the values of the carrier frequency and the frequency of the probing signal deviation, at which there are no distortions of the signal spectrum, are obtained. Examples of numerical calculations are given that confirm the validity of the obtained relations.

This article was written during the implementation of Research & Development work on the topic: "Creating a scientific and technical reserve in the field of building a unified miniature airborne radar target load of small-sized unmanned aerial vehicles for monitoring ice conditions during the construction and operation of oil and gas platforms".

Agreement № 14.577.21.0226. The unique identifier of Research & Development: RFMEFI57716X0226.

### References

- Ananenkov, A.E., Kanaschenkov, A.I., Nuzhdin, V.M., Rastorguev, V.V. & Smolyar, A.M. (July, 2017). Estimation of potential characteristics of onboard radar for ice surface monitoring, International Conference on Transparent Optical Networks ICTON-2017, Girona, Catalonia, Spain.
- Batet, O., Dios, F., Comeron, A. & Agishev, R. (2010). Intensity-modulated linear-frequency-modulated continuous-wave lidar for distributed media: fundamentals of technique. Optical Society of America, 49(17), 3369-3379.
- Gavrilov, K.Yu., Kanaschenkov, A.I., Nuzhdin, V.M. & Panyavina, N.S. (2018). Signal processing during the synthesis of aperture in a radar with continuous radiation. Information-measuring and control systems, 16(6), 31-46.
- Gonorovsky, I.S. (1986). Radio circuits and signals. M.: Radio and communication.
- Komarov, I.V. & Smolsky, S.M. (2010). Fundamentals of the theory of radar systems with continuous radiation of frequency-modulated oscillations. M.: Hotline - Telecom.
- Kanashchenkov, A.I., Matveev, A.M., Minaev, E.S. & Novikov, S.V. (2017). New Generation Compact Integrated Radar Systems for Aerial Vehicles. Russian Aeronautics, 60(4), 647-652.